PROCEEDINGS OF THE INTERNATIONAL CONFERENCE NANOMATERIALS: APPLICATIONS AND PROPERTIES
Vol. **1** No 2, 02NFC34(3pp) (2012)

Formation of Superhard Nanostructured Ti–Hf–N(Fe) Coatings Obtained by Vacuum Arc Deposition in HF discharge

A.D. Pogrebnyak[1,*], A.G. Ponomarev[2], M. V. Kaverin[1], D.A. Kolesnikov[3], V.M. Beresnev[4], O.V. Bondar[1], S.S. Mel'nik[5], T.N. Koltunowicz[6]

[1] *Sumy State University, 2, Rymsky Korsakov Str., 40007 Sumy, Ukraine*
[2] *Institute of Applied Physics, NAS of Ukraine, 58, Petropavlivska Str., 40030 Sumy, Ukraine*
[3] *Belgorod State University, 85, Pobeda Str., 308015 Belgorod, Russia*
[4] *Kharkiv National University, 21, Frunze Str.,61002 Kharkiv, Ukraine*
[5] *Belarusian State University,4, Nezavisimosti Ave., 220030 Minsk, Republic of Belarus*
[6] *Lublin University of Technology, 38A, Nadbystrzyska Str., 20-618 Lublin, Poland*

(Received 11 July 2012; published online14 August 2012)

Superhard nanostructured Ti–Hf–N(Fe) coatings are prepared. The formation of local regions of (Ti, Hf)N, FeN, and Hf is detected using μ-PIXE (ion microbeam). It is revealed that the synthesized coatings have a nanohardness of 48 ± 1 GPa and are composed of nanograins with a size of 4.8–10.6 nm, which are enveloped by finer entities of other phases (Ti, Fe)N and FeN. There is a good correlation between the results derived by XRD, TEM, AFM, and SEM and microanalysis, which in turn are complemented by the analysis results obtained using an ion microbeam and PIXE.

Keywords: Superhard, nanostructured, Ti–Hf–N(Fe), μ-PIXE, ion microbeam, nanohardness,

PACS number(s): 61.46 – w.62.20.Qp, 62.25. – q

1. INTRODUCTION

It is known that the unique properties of nanostructured nanocomposite coatings are a high volume fraction of the interfaces and their strength, the absence of dislocations inside the crystallites, the possibility of changing the ratio of fractions of thevcrystalline and amorphous phases, and the mutual solubility of the metallic and nonmetallic components [1–3]. For example, the presence of a large area of the interface (the volume fraction of which can achieve ≥ 50%) in nanostructured films and coatings makes it possible to significantly change their properties both by modifying their composition and electronic structure and by doping with various elements. The strength of the interface contributes to an increase in the strain resistance of nanostructured coatings, and the absence of dislocations inside the crystallites increases the elasticity of the coatings. Therefore, it is a high priority problem of materials science and solid state physics to study the physical causes of the high physicomechanical properties of nanostructured materials (coatings).The formation of local regions of Al and C upon the implantation of Al ions into α-Fe owing to segregation and the formation of a helicoid was found in [3, 4] using an ion microbeam, positron annihilation, and electron microscopy; enhancement of the diffusion of N^+ ions during ion-plasma modification was shown in [5]. Thus, the objective of this Letter is to analyze the effect of segregation and mass transfer processes on the formation of nanosized regions and the effect of changes in the interface on superhardness. Ti–Hf–N(Fe) films with a thickness of 1.5 μm were deposited on steel samples with a diameter of 20 and 30 mm and a thickness of up to 3 mm in a vacuum chamber using a vacuum arc source in a high-frequency (HF) discharge and employing a Ti–Hf(Fe) cathode (sintered by an electron gun in an Ar atmosphere). To obtain nitrides, we filled the chamber of the setup with atomic N at different pressures and substrate potentials. The deposition parameters are listed in the Table 1.

2. EXPERIMENT AND DISCUSSION

To analyze the properties of the Ti–Hf–N(Fe) coatings, we used a scanning nuclear microprobe based on an electrostatic accelerator designed at the Institute of Applied Physics, National Academy of Sciences of Ukraine [6]. Analysis was performed using Rutherford backscattering (RBS) and proton induced characteristic X-ray emission (PIXE and μ-PIXE) at an initial energy of E_p = 1.5 MeV, a beam size of 2-4 μm, and a current of $\approx 10^{-5}$ A [5]. The total PIXE spectrum was analyzed using the GUPIXWIN software, which provided information on the quantitative content of elements and stoichiometry. To compare the elemental composition and to analyze the morphology, we used a Quanta 200 scanning electron–ion microscope with an EDS detector. A Bulat-3T vacuum arc source with an HF genera tor was used [8]. A bias potential was applied to the substrate from the HF generator, which generated decaying oscillation pulses at a frequency of ≤1 MHz, Ti–Hf–N(Fe) coating deposition parameters; crystallite sizes and hardness for different sets of samples. (The calculation was carried out by Vegard's law according to solid-solution period values; the effect of macrostresses on the diffraction line shift was not taken into account) a pulse duration of 60 μs, and a repetition frequency of 10 kHz.

* alexp@i.ua

Table 1 – Deposition parameters and coatings characteristics of Ti–Hf–N(Fe)

No.	P, nitrogen pressure in the chamber, Pa	Substrate potential, V	Nano-hardness, GPa	Average crystallite size, nm
7(direct) 11 (separated)	0,3 0,5	-200 -200	41.82 47.17	6.4 4.8

The negative substrate auto-bias voltage, owing to the HF diode effect, was 2–3 kV. In addition, we used an RBS scheme with 1.3-MeV He^+ ions, a registration angle of $\theta = 170°$, and a detector resolution of 16 keV. The dose of helium ions was ≈5 μs [5].

XRD analysis of the nanostructured films was carried out using two diffractometers: DRON-4 and X'Pert PANlytical (Holland) with a step size of 0.05° at a tube voltage of $\mathcal{U}$ = 40 V and a current intensity of $\mathcal{I}$ = 40 mA; the emitter was copper $Cu\mathcal{K}_\alpha$. The analysis of morhology, structure, and elemental composition on the cross sections of the coatings was performed using a Quanta 200 3D scanning electron–ion microscope. The mechanical properties—i.e., hardness, nanohardness, and elastic modulus—were studied using two Nanoindentor G 200 instruments (MES System, United States) employing Berkovich and Vickers pyramids; in addition, we employed a Rockwell C indenter with a radius of curvature of about 200 μm. Figure 1 shows the distribution maps for the elements in the coating, which were obtained using an ion microbeam, depending on color (dark regions with a low concentration, lighter regions with a high concentration of elements).

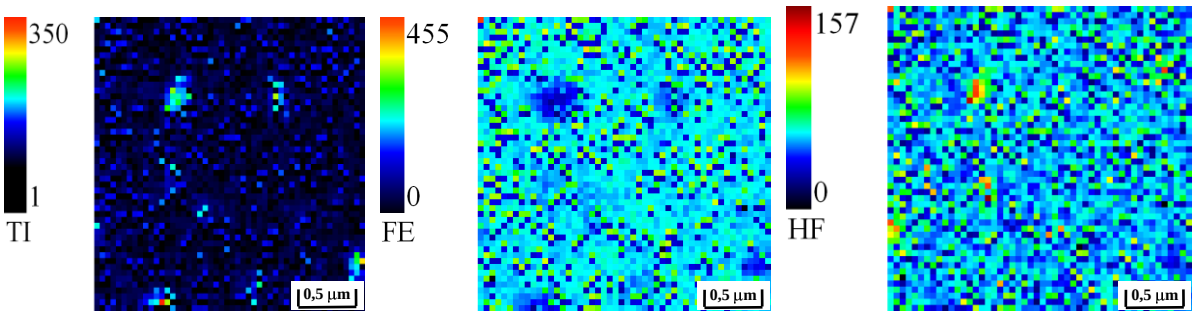

Fig. 1 – Element (Ti; Hf; Fe) distribution maps derived for the steel samples with a deposited Ti–Hf–N(Fe) coating. In particular, there are local regions with sizes of from 2–4 to 6–10 μm that consist of Hf and Ti inclusions, in which the concentration of Fe dramatically decreases

It is evident from these figures that the coatings exhibit a certain heterogeneity of the surface and depth distribution of the Ti, Hf, and Fe elements. The PIXE-derived quantitative analysis and its stoichiometry are represented in Fig. 2. The results (the concentration integrated over depth is about 2 μm) show that a thin AlC film is formed on the surface, which is probably the result of exposure to a proton beam, and the main concentration of the elements is as follows, at %: Fe ≈ 77, Ti ≈ 11, Hf ≈ 11.05, Mn ≈ 0.9, and Cr =0.01; the last-mentioned elements apparently are part of the substrate.

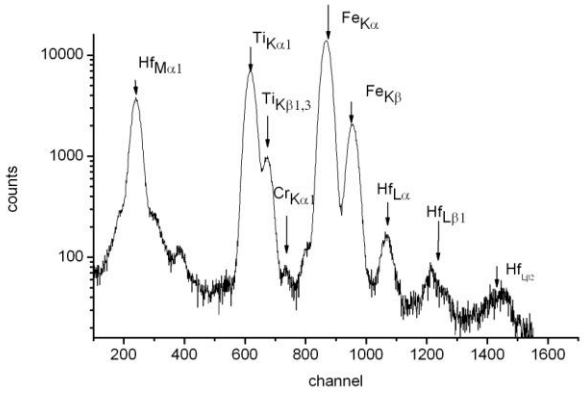

Fig. 2 – Total PIXE spectrum (in a logarithmic scale) derived from the sample with an Hf–Ti–N–Fe coating in the analysis using a 1.5-MeV proton beam (the spectrum was recorded using a silicon detector)

Figure 3b depicts an image of a region of the surface area of the coating with the imprint of the indenter, which is equivalent to the nanohardness of 48 ±1 GPa; this nanohardness value is very high about 50 GPa—and, according to the modern classification scheme, corresponds to a superhard coating. At the same time, the nanohardness of the coating measured using a Vickers pyramid is 36.4 GPa, because a softer steel substrate is located under the coating (Fig. 3b). The XRD analysis results obtained for the samples with this coating type show that the coatings are composed of at least two phases (Ti, Hf)N, (Ti, Hf)N, or FeN and the nanograin sizes determined from the diffraction peak widths by the Debye–Scherrer technique are 4.8–10.6 nm. TEM analysis revealed that a mixture of phases is formed in the coating: a nanocrystalline (Ti, Hf)N phase with a grain size of 3.5–7.2 nm and a quasiamorphous phase, which is apparently FeN; that is, there is a good correlation between the data of XRD and TEM analyses, which show that the nanograin sizes have approximately the same order of magnitude. In addition, by changing the coating deposition parameters, we can specify the stoichiometry (composition) of the film; that is, by changing the substrate potential of 0, –100, and –150 to –200 V, at the same pressure of nitrogen (or an Ar/N mixture), we can change the coating structure from columnar (Fig. 3a) at low pressures to nanograin at a high potential. Three dimensional islands on the surface of the films with a columnar structure emerge on the surface of the faces of individ-

ual grains (Fig. 3a). It is evident that the surface roughness depends on chemical composition and on deposition parameters. Surface undulation is attributed to the growth mechanism and the formation of individual islands on the surface (Volmer–Weber mechanism). In addition, measurement of the XRD spectra in the coating in the θ–2θ geometry and the $\sin^2\varphi$ method revealed compression microstresses, which are formed in nanograins and correspond to a compression value of ≈2.6%. The compression stresses that occur in the film growth plane, which were measured according to the position of the diffraction line peaks by the $\sin^2\varphi$ method, were ≈2.78%.

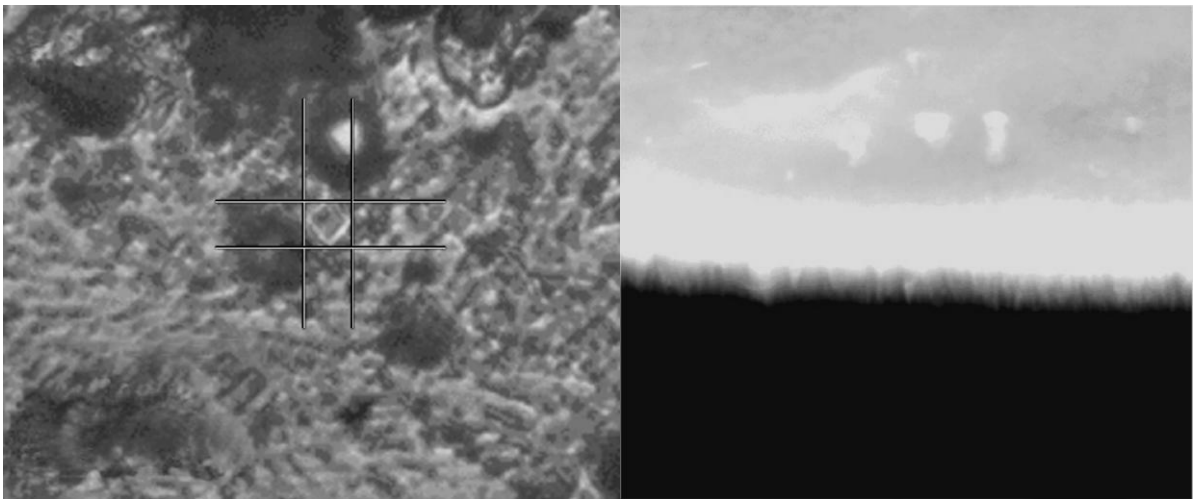

a) b)

Fig. 3 – (a) Cross section of the Hf–Ti–N–Fe coating with a columnar structure; (b) imprint of a four-sided Vickers pyramid on the Ti–Hf–Fe–N coating with a nanohardness of H_V = 36.4 GPa

Upon the separation of a plasma beam, the resulting coatings are textured to varying degrees; for example, in the case of a high potential applied to the substrate (–100 V), we have a texture with the [110] axis.

In addition, note that, in the nontextured fraction of the crystallites, their average size is about 5.8 nm, while it is significantly higher in the textured fraction and achieves 10.8–12 nm. It was shown in theoretical studies that, in the case of formation of nanocomposites with TiN-nc and α-Si_3N_4 (in the form of a quasiamorphous phase) with a thickness of less than 1 nm (approximately a monolayer), the resulting coatings exhibit a very high hardness (superhardness) up to 80 GPa [5]. A necessary and sufficient condition for this is the completion of the spinodal grain-boundary segregation; however, this requires a high substrate temperature during deposition (600–650ºC) or fairly high diffusion rates; since the substrate temperature during deposition in our case did not exceed 300 ºC, the spinodal segregation process was apparently not completed [4].

The represented distributions of elements over the coating surface and to a depth of 2 μm (i.e., in the 3D geometry) show that, in fact, the segregation process has not been completed; therefore, the derived hardness values of ≈50 GPa can be increased (by 15–25%) owing to rapid diffusion and the completion of the spinodal segregation process [4, 5]. That is, we can state that the "self-hardening" effect in superhard coatings can lead to an increase in nanohardness up to 60–65 GPa. The μ-PIXE results imply that, apparently, it will be possible to control the self-hardening process or the grain-boundary diffusion acceleration and, thereby, to in situ control the spinodal segregation and the distribution of elements.

ACKNOWLEDGMENTS

Authors thank O.V. Sobol' (Kharkiv Technical University) for help in interpreting the XRD analysis results. This work was supported by the State Foundation for Basic Research of Ukraine (project F-41/20-2011) and the Belarusian Republic Foundation for Basic Research (project T11K-058).

REFERENCES

1. A.D. Pogrebnyak, A.P. Shpak, V.M. Beresnev, N.A. Azarenkov, *Phys. Usp.* **52**, 29 (2009).
2. R.A. Andrievskii, A.M. Glezer, *Phys. Usp.* **52**, 315 (2009).
3. A.D. Pogrebnyak, A.P. Shpak, V.M. Beresnev, et al., *Tech. Phys. Lett.* **37**, No7, 637 (2011).
4. A.D. Pogrebnjak, V.M. Beresnev, A.P. Shpak et al., *Rus. Phys. J.* **54** No11, 1218 (2012).
5. G. Abrasonis, W. Moller, Xin Xin Ma, *Phys. Rev. Lett.* **99**, 065901 (2006).